



This is a repository copy of *Numerical investigation of buoyancy-driven heat transfer within engine bay environment during thermal soak*.

White Rose Research Online URL for this paper:
<https://eprints.whiterose.ac.uk/175294/>

Version: Accepted Version

Article:

Yuan, R., Sivasankaran, S., Dutta, N. et al. (2 more authors) (2020) Numerical investigation of buoyancy-driven heat transfer within engine bay environment during thermal soak. *Applied Thermal Engineering*, 164. 114525. ISSN 1359-4311

<https://doi.org/10.1016/j.applthermaleng.2019.114525>

Reuse

This article is distributed under the terms of the Creative Commons Attribution-NonCommercial-NoDerivs (CC BY-NC-ND) licence. This licence only allows you to download this work and share it with others as long as you credit the authors, but you can't change the article in any way or use it commercially. More information and the full terms of the licence here: <https://creativecommons.org/licenses/>

Takedown

If you consider content in White Rose Research Online to be in breach of UK law, please notify us by emailing eprints@whiterose.ac.uk including the URL of the record and the reason for the withdrawal request.



eprints@whiterose.ac.uk
<https://eprints.whiterose.ac.uk/>

Title:

Numerical investigation of buoyancy-driven heat transfer within engine bay environment during thermal soak

Author names and affiliations

Ruoyang Yuan¹, ¹Aeronautical and Automotive Engineering, Loughborough University
Address: Stewart Miller Building Loughborough University, Loughborough LE11 3TU
Email: r.yuan@lboro.ac.uk

Sureshkumar Sivasankaran², ²Thermal & Aerodynamic Systems Engineering, Jaguar Land Rover
Address: B540, TASE, JLR, Gaydon, Warwick, CV35 0RR
Email: ssures15@jaguarlandrover.com

Nilabza, Dutta², ²Thermal & Aerodynamic Systems Engineering, Jaguar Land Rover
Address: B540, TASE, JLR, Gaydon, Warwick, CV35 0RR
Email: ndutta@jaguarlandrover.com

Wilko Jansen², ²Thermal & Aerodynamic Systems Engineering, Jaguar Land Rover
Address: B540, TASE, JLR, Gaydon, Warwick, CV35 0RR
Email: wjansen5@jaguarlandrover.com

Kambiz Ebrahimi¹, ¹Aeronautical and Automotive Engineering, Loughborough University
Address: Stewart Miller Building Loughborough University, Loughborough LE11 3TU
Email: K.Ebrahimi@lboro.ac.uk

Corresponding author

Ruoyang Yuan

Email: r.yuan@lboro.ac.uk

Please refer to the published journal article here: <https://doi.org/10.1016/j.applthermaleng.2019.114525>

© 2019 Elsevier Ltd. This manuscript version is made available under the CC-BY-NC-ND 4.0 license

<http://creativecommons.org/licenses/by-nc-nd/4.0/>

Title: Numerical investigation of buoyancy-driven heat transfer within engine bay environment during thermal soak

R. Yuan^{1,*}, S. Sivasankaran², N. Dutta², W. Jansen², K. Ebrahimi¹

¹: Aeronautical and Automotive Engineering, Loughborough University, Loughborough, LE11 3TU, UK

²: Thermal & Aerodynamic Systems Engineering, Jaguar Land Rover, Gaydon, Warwick, CV35 0RR

*: Corresponding author, e-mail: r.yuan@lboro.ac.uk

Abstract—This paper investigates transient heat transfer processes of a vehicle under-bonnet region during natural soak condition using computer aided engineering (CAE). Heat reserved within the engine bay is beneficial to the engine cold-start for potentially reductions in friction losses, CO₂ emissions and fuel consumption. Buoyancy-driven convection, thermal radiation and conduction are key contributors to heat transfer processes of engine compartments during soak. In this study, a coupled transient 3D computational fluids dynamics (CFD) – heat transfer modelling method was studied in a passenger vehicle to simulate its 9 hours cool-down behaviours. The developed CAE method was able to predict the temperature cool-down of the key fluids of good agreement with experiments. Potential air and heat leakage paths around the engine bay were identified. The flow development during the early stage (0-2 hrs) of the soak was vital to accurate prediction of the heat transfer coefficients for the heat retention modelling, where convection and radiation have played important parts. Optimum simulation strategy was obtained with reduced simulation time and good prediction accuracy. This further allows the integration of engine encapsulation design for optimising fuel consumption and emissions in a timely and robust manner, aiding the development of low-carbon transport technologies.

Keywords— ATCT/WLTC driving cycle, buoyancy-driven heat transfer, CAE method, heat retention modelling, vehicle thermal soak.

Highlights

- 3D CFD modelling of buoyancy-driven convection flow resolved on full-geometry vehicle
- Convective heat transfer coefficients characterised during natural soak environment
- Coupled transient CFD - heat transfer modelling analysis was demonstrated
- 9 hrs cool-down behaviours of the key engine fluids were resolved
- A CAE tool developed enabling evaluations of heat retention and encapsulation design

Declarations of interest: none

1. INTRODUCTION

The continuous improvement of fuel consumption and reduction of CO₂ emissions are key deliverables for the modern vehicle designs to meet the tightening worldwide emissions standards and related regulations. With the introduction of the supplemental Ambient Temperature Correction Test (ATCT) in the World-wide harmonised Light duty Test Procedure (WLTP) driving cycle [1], the vehicle is placed under static soak condition for 9 hours in between the first and second WLTP test cycles under the ambient temperature conditions of 23°C and 14°C respectively. If the heat can be preserved in the engine bay during the 9 hrs static soak period, the temperatures of the fluids (engine oil, transmission oil, and engine coolant) could be increased at the start of the second WLTP cycle. This favours the friction loss reduction during the engine warming-up process, which further provides benefits on both CO₂ emissions and fuel economy. To retain the heat within the engine bay during the vehicle soak, under-bonnet thermal encapsulation was used [2] to keep the temperatures within the engine compartment. This study reported that the encapsulation alone reduced fuel consumption by up to 0.2% for each extra degree of temperature (in °C) retained. In a previous research project joint by Jaguar Land Rover and Autoneum [3], it was found that the under-bonnet thermal encapsulation had the potential to retain the fluid temperature of 9 °K and 11 °K in the coolant and oil respectively after a four-hour vehicle soak period. This further led to a 2.3% CO₂ saving benefit on a full WLTP cycle carried out in the reported work [3]. It is thus desirable to further optimise and embed the thermal encapsulation design together with the thermal analysis into vehicle design process to allow the vehicle performance assessments occur at the early stages of the development cycle.

The thermal modelling and analysis with the computer aided engineering (CAE) have the potential to predict the essential fluid

and engine components' cool-down behaviours and have the capability to visualise the thermal and air leakage paths of the engine bay during the 9 hrs thermal soak phase, thus play a critical role in the under-bonnet thermal encapsulation design. When vehicle undergoes soak stage, the air flow and the associated convective heat transfer around and within the engine bay are driven by the buoyancy effect. In the buoyancy flow, a non-dimensional parameter is usually used to correlate heat and mass transfer due to thermally induced natural convection, which is often described by the Grashof number, Gr , as defined in (1).

$$Gr = g\beta\Delta TL^3\nu^{-2} \quad (1)$$

where g is the acceleration due to gravity, β is the thermal expansion coefficient, ΔT is temperature difference between the averaged surface and the bulk of the fluid, L is the representative dimension and ν is the kinematic viscosity of the fluid. Grashof number represents the ratio between the buoyancy and viscous forces of the fluid. Similar to the role that Reynolds number plays in forced convection, Grashof number is used to categorise the flow regimes as laminar, transition and turbulent in natural convection. The critical Gr is about 10^9 for vertical plates, above which the flow becomes turbulent. Grashof number is often used as an important parameter to quantify the heat transfer. The heat transfer coefficient h is often obtained by (2) from the Nusselt Number Nu , which is a function (3) of Prandtl Number Pr and Grashof Number Gr in natural convection.

$$h = (Nu \cdot k)/L \quad (2)$$

$$Nu = f(Ra, Pr) = f(Pr \cdot Gr, Gr) \quad (3)$$

where k is the thermal conductivity of the fluid. Ra , the Rayleigh number, is the product of Pr and Gr . For a vertical plate, Nu is expressed in (4).

$$Nu = \begin{cases} 0.59 (Ra)^{1/4} & 10^4 < Ra < 10^9 \\ 0.1 (Ra)^{1/4} & 10^9 < Ra < 10^{13} \end{cases} \quad (4)$$

Chen et al. [4] numerically investigated the buoyancy-driven flow structure in a simplified under-bonnet model with open enclosure mimicking the under-bonnet soak condition. A simplified engine block and exhaust cylinders were included to represent the heat sources. The Grashof numbers used in this study were around 3×10^8 and 4×10^5 at the nearby regions of the engine block and exhaust respectively. The transient simulation was carried out using ANSYS Fluent [5]. The transient simulation with time-steps from 0.01 s to 0.001 s was run for 60 seconds of physical time before reaching a steady state result. The computing power used in this study was 32 CPUs with total running time of 12 and 85 hours for the coarse (with mesh size of 5 mm) and fine (of 1 mm) mesh cases, respectively. The buoyancy-driven flow and temperature fields modelled were compared with measurement data by particle image velocimetry and thermocouples [6]. An overall good agreement was found in the air velocities and engine block wall temperatures, although some discrepancies were observed in one side of the block attributed to the less restricted space that promoted larger recirculating motion calculated from the simulation [4]. It was emphasised that the transient numerical approach was necessary to obtain meaningful buoyancy driven flow solution. Although buoyance-driven air flow was well evaluated, the heat transfer to the metal parts and the heat transfer from the metal parts to the internal fluids were not in the scope of the reported study.

To evaluate the heat retention during the soak stage for the vehicle, the buoyance-driven convection as well as thermal radiation and conduction heat transfer to the metal and internal fluids are the key factors to the thermal simulation of the engine bay. These affect the accurate predictions of fluids temperature trajectories during the vehicle cool-down. This further affects the numerical predictions of the CO₂ emissions and fuel consumption during the second 14°C cold-start WLTP drive cycle. However, to numerically model the under-bonnet region during soak condition in a full-size vehicle requires a significant amount of computer resources and techniques.

Upon the studies on the simplified engine bay geometry [4-7], the transient simulation method for the buoyance-driven convection flow in the engine bay was developed further to apply in passenger vehicles for unsteady thermal management [8-10]. Numerical investigations [8] were carried out combining 3D computational fluid dynamics (CFD) simulation from STAR-CCM+ with 1D thermal modelling in GT-SUITE for the heat retention analysis in an engine bay with thermal encapsulation of a Volvo S80 passenger car. The mass-flow and thermal distribution over the cooling package were simulated in several steady-state operating points by the CFD with a number of vehicle and fan speeds, and the results from which were imposed on a 1D underhood model in GT-SUITE at both steady-state and transient conditions. 600 CPU hours was used for most cases of the steady-state 3D CFD [8]. The buoyancy-driven flow and the heat retention in an engine bay with engine thermal encapsulation of a Volvo S80 passenger car was further on numerically investigated with the integrated 1D-3D approach in an iterative process to evaluated the potential benefit on engine friction reduction in applications with frequent cold starts [9]. The 3D CFD was initialised with the temperatures of engine solids calculated at the end of the 1st WLTP cycle by the 1D engine thermal model in GT-SUITE. Heat

transfer coefficients computed by the steady 3D CFD simulation of buoyancy-driven flow were fed into the 1D thermal representation of heat conduction in the engine solids. Next, a 1D engine thermal simulation was started for 20 second physical time, during which the heat transfer coefficient due to natural convection and radiation were taken as constant. Following the transient heat transfer 1D modelling, the temperature of solids were updated and re-mapped onto the 3D models to calculate the buoyancy flow. A WLTP drive-cycle vehicle simulation and consequently fuel consumption analysis were implemented in GT-SUITE with sub-models including a 1D longitudinal vehicle dynamic model and 1D mapped engine performance model. It reported a 2.5% and 1.5% fuel savings for engine-starts occurring 2 to 8 hours after key-off at ambient temperature 5°C and 20°C separately for encapsulation with high degree (97%) of coverage. A comparison between measured and simulated coolant and oil temperatures were plotted with overall good correlation for 20 min cool-down duration after the key-off event, with some discrepancy observed due to the 1D thermal engine model unable to predict the flow and heat transfer in the coolant jacket at low flow rates. A validation of the simulated temperatures of the fluids against the testing data was not provided in the reported study for the complete 9 hrs soak condition. This adds uncertainty to the prediction of the fuel consumption saving for the second WLTP drive cycle. The computing resource used in this study [9] was 24,000 CPU-hours for a 16 hours simulated drive cycle.

A recent 3D thermal CFD work on under-bonnet heat retention analysis during vehicle soak were carried out on a Range Rover Evoque vehicle with comparison of the testing data for the complete 9 hours soak period with and without encapsulation [10]. The CAE tools applied in this study were PowerFLOW and PowerTHERM supplied by SIMULIA. A coupled process was adopted in which the buoyancy-driven flow was transiently solved from PowerFLOW coupled with a full-geometry heat transfer solver PowerTHERM. The fluids temperature cool-down trajectories of the coolant and oil were obtained and compared with the testing data. In general, good correlations were found in between the CAE results and the test results. Further improvements required to improve the cool-down curve offset and to extend the work to evaluate the engine second cold-start benefits. The computing resources required in this coupled 3D thermal CFD work adopted in this study for the transient thermal analysis was high, for which a total 258,000 CPU-hours was used.

To be embedded into the early vehicle design stage, it is required that the CAE method takes account of the complexity of the designed geometries and is able to accurately model the buoyancy-driven transient heat transfer process as well as the thermal radiation and conduction process. The challenge of the CAE modelling for the thermal modelling of the vehicle under the soak comes with the trade-off in between the computing cost and the prediction accuracies of the key fluids temperatures. In this paper, we investigate the software integration for simulations of buoyancy-driven heat transfer in a vehicle under-bonnet during thermal soak. The 3D under-bonnet flow dynamics were solved inherently transient by the Lattice-Boltzmann Method (LBM) method [11] using CFD and coupled with detailed heat transfer modelling using a thermal solver. The particle-based LBM method was capable of accurately handling extremely complicated surface geometries. The detailed thermal modelling including heat conduction, radiation and buoyancy-driven heat convection were integrated solved by the thermal solver. The 9 hrs cool-down period was simulated using a combination of coupled transient and fast transient modelling process, and compared with the vehicle testing data of the key fluids (coolant, oil) temperatures. The coupling method, sensitivities of the internal and external heat transfer coefficients to the CAE results, the potential reduction of the computing time formed the focus of this work. Heat transfer contribution from convection, conduction and radiation during the 9 hrs soak were evaluated.

2. NUMERICAL METHODS

2.1. Flow field modelling by Lattice-Boltzmann Method

To model the unsteady buoyancy-driven flow behaviour under vehicle soak conditions, the Lattice-Boltzmann Method (LBM) was used provided by PowerFLOW, SIMULIA. Different from the traditional CFD approach via solving the Navier-Stokes equations that statistically describe a real fluid, the LBM, based on Digital Physics technology, models fluid at a more fundamental kinetic level using a discrete Boltzmann equation. The Boltzmann equation governs the dynamics of particle distribution functions. The Lattice Boltzmann Equation with the Bhatnagar-Gross-Krook (BGK) approximation [12] is expressed in (5).

$$f(\vec{x} + \vec{\xi}, t + 1) - f(\vec{x}, t) = -\frac{1}{\tau} [f(\vec{x}, t) - f^{eq}(\vec{x}, t)] \quad (5)$$

where $f \equiv f(\vec{x}, \vec{\xi}, t)$ describes the single particle number density f at time t and position \vec{x} with velocity $\vec{\xi}$. τ is the relaxation time due to collision, and f^{eq} stands for the equilibrium distribution, described by the Maxwell-Boltzmann distribution function:

$$f^{eq} \equiv \frac{\rho}{(2\pi RT)^{\frac{D}{2}}} \exp \left[-\frac{(\xi - \bar{u})^2}{2\theta} \right] \quad (6)$$

in which R is the gas constant, D is the dimension of the space, θ is the normalised temperature given by $\theta = k_B T/m$. k_B , T , m are the Boltzmann constant, temperature and particle mass separately. \bar{u} is the macroscopic hydrodynamic velocity. LBM tracks the motion of macromolecules through space and time to simulate flows of gases and liquids. It inherently conserves mass, momentum and energy to simulate fluid behaviour. The macroscopic hydrodynamic quantities are direct results of the moments of

particle density distributions given by:

$$\begin{aligned}\rho &= \sum_i f_i(\vec{x}, t) \\ \rho \vec{u} &= \sum_i \vec{u}_i f_i(\vec{x}, t) \\ \rho \varepsilon &= \sum_i \frac{1}{2} (\vec{\xi}_i - \vec{u})^2 f_i(\vec{x}, t)\end{aligned}\quad (7)$$

where ρ , \vec{u} , and ε are the mass density, the velocity and the internal energy density, respectively. Three microscopic processes were used in LBM to simulate the fluid behaviour include particle to particle interactions, particle to surface interactions and advection particle movement. The Lattice Boltzmann model used in Digital Physics [11], particles exist at discrete locations in space, shown in the diagram (Figure 1) where particles reside on a cubic lattice composed of voxels and surfels. Surfels are surface elements that occur where the surface (of which geometry can be arbitrary) of a body intersects the fluid. During the simulation, particles interact as they move from voxel to voxel during discrete intervals of time with discrete speeds. The particle density distribution functions are tracked when millions of particles move in each direction at each voxel. Particles in the same voxel collide and change speed and/or direction while conserving total mass, momentum and energy in the voxel (particle to particle interactions and advection). For the particle to surface interactions and advection, particles that would hit a surfel within a timestep are first gathered by the surfel. The surface-collision process enforces the conservation of mass while exchanging momentum and energy with desired boundary condition specification. The amount of momentum change corresponds to pressure and friction. After the above described voxel-to-surface advection process, the gathered particles are reflected and returned to the fluid voxels. The key characteristics of the LBM are: (1) it is an efficient unsteady flow solver and with low numerical dissipation, (2) it is capable to handle very complex geometries and (3) it uses Very Large Eddy Simulations (VLES) turbulence model including subgrid modelling and wall-function modelling. Turbulence in the anisotropic turbulent scales (or very large eddies) is directly resolved, while turbulence in the dissipative and inertial ranges is modelled [11, 13].

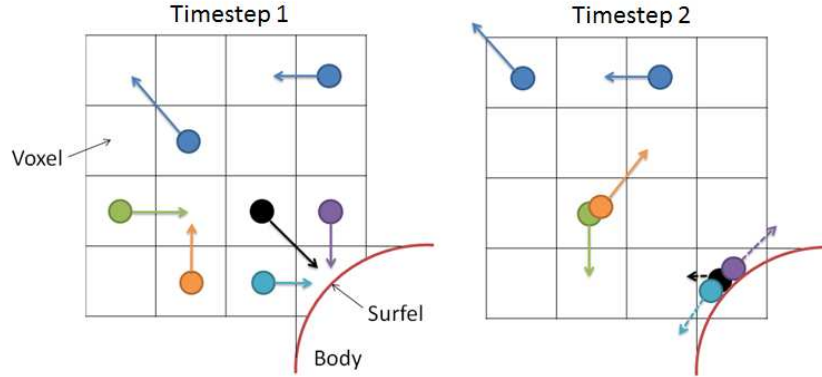


Fig. 1 Diagram of the particle/surfaces

Aside from solving for the aerodynamic flow behaviours, the buoyancy-driven convection was also solved by CFD. The Heat transfer coefficients (HTCs) from the convection were derived from heat flux q , surface temperature T_{wall} and a reference temperature (either near wall temperature or characteristic temperature) T_{ref} using (8),

$$HTC = q / (T_{wall} - T_{ref}) \quad (8)$$

except that the near wall HTC in turbulence modelling simulations was calculated using the turbulent thermal wall model [11].

The near wall temperatures and HTCs calculated from CFD were seeded into the thermal solver as boundary conditions to solve thermal conduction and radiation.

2.2. Heat Transfer Modelling

The thermal modelling of the engine bay during vehicle soak was solved using PowerTHERM®, which is a heat transfer analysis program that predicts surface temperatures and heat fluxes generated by heat radiation, conduction and convection [14]. Temperature of the components are influenced by all means of heat transfer, such as the radiation from the exhaust line, the conduction from the engine metal part and the convection from either fan driven initially followed by buoyancy-driven flow latterly. The radiation heat transfer was automatically calculated through View Factors. Conduction was solved based on geometry connectivity, material properties and special part types, such as fluid, fluid stream, and lumped capacitance. The engine geometry

was represented as shells with the metal mass themselves being represented as lumped masses and with a fluid node representing the fluid volume (coolant or oil) residing within the metal mass. Convections in between the surrounding air to the metal components were solved using the near wall fluid (i.e. air) temperatures and fluid HTC values imported from the CFD simulation. Convections in between metal part to the internal fluids (coolant and oil) were calculated with assigned internal HTC values. Note here that the assigned internal HTC values were not from the CFD calculations, but were obtained from a correlated 1D GT-SUITE model. The sensitivity of the internal HTC values to the thermal transient modelling and the resulted cool-down behaviours were investigated in this study.

2.3. Coupled Simulation Approach

A coupled aerodynamic flow - heat transfer modelling was carried out using CFD and a thermal solver to simulate thermal cool-down behaviour of the engine bay during the vehicle soak condition. In the coupled thermal simulation, the heat exchange at all of the surfaces was computed by the thermal solver. The fluid flow, fluid temperatures and HTCs were computed by the CFD simulation. The wall temperatures were used as an isothermal boundary condition in the CFD simulation while the convection HTCs and fluid temperatures computed by the CFD were used as convection boundary conditions in the thermal solver. The simulation process is illustrated in figure 2. A steady state thermal solution was first obtained with the thermal solver for the surface (wall) temperatures as the input to the flow solver to initiate the coupled transient simulation. During the coupled transient simulation stage, the two solvers were running in parallel and were exchanging data frequently at a user-defined time interval Δt . There would be a balance in between the time interval (Δt), the physical time (t_{couple}) set for the transient couple simulation stage, and the computing resources. Ideally t_{couple} is set for the entire soak period of 9 hrs with the finest Δt to simulate heat transfers during the cool-down event, however the computing will be very resource intensive and not cost-effective. It is also noteworthy that the nature convection due to buoyance is negligible compared with heat transfer from conduction in the later stage of the soak. Thus, a fast transient was used with thermal solver standalone to obtain the thermal solution for the rest of the cool-down period. The sensitivity of the t_{couple} period to the final thermal solution was investigated in this study and will be discussed in the result section.

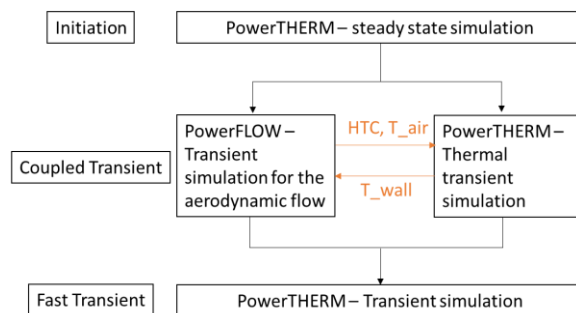


Fig. 2 Diagram of the thermal transient simulation process

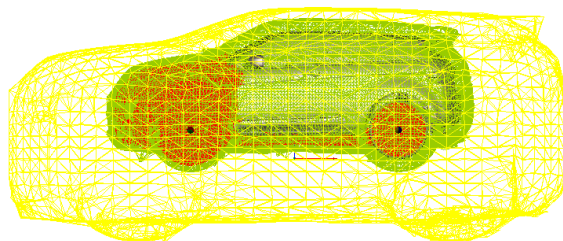


Fig. 3 Example of variable voxel resolution regions for the external flow

In PowerFLOW, variable mesh resolution regions were used to specify regions of lattice refinement. In current cases, finer meshes were placed in the flow areas nearer to the surface of solid surfaces, and after impediments to internal flow. Figure 3 shows the visualised region of meshes refined closer to area of interest for computational benefit without compromising accuracy. In the current flow simulation, 1 time-step equalled 0.661 ms of physical time. The Reynolds number was 186.4 and fluid Prandtl number was 0.707.

2.4. Data Correlation and Analysis

The CAE results were compared with the test data of the key fluids cool-down curves. The test set up can be referred to [10]. In this paper, the modelling methodology was investigated to study the optimum cool-down predictions with reduced computing resources. The sensitivities of the predict cool-down behaviours from CAEs are examined with various internal fluids HTCs,

external HTC and coupling time t_{couple} . The relative contribution of the heat transfer to the engine components from radiation, convection and conduction were also evaluated.

3. RESULTS AND DISCUSSIONS

3.1. Flow field visualisation at beginning of the soak

At the beginning of the 9 hours vehicle soak, the external and internal flows surrounding the vehicle engine bay were resolved from the coupled simulation. Figure 4 shows the streamlines of the flow field superimposed on the flow temperature result (normalised by the maximum temperature) around the engine bay at the timeframe of 0 s, 5 min and 10 min of the soak. It indicates that the internal flow near the heat sources (e.g. exhaust lines, engine block) was initially heated up (Figs 4a-b) and then dropped gradually (Fig 4c). It induced vortexes formation and their associated movements within the engine bay. Figure 5 indicates the flow velocity magnitude and the fluid temperature within the under-bonnet region and around the vehicle at the timeframe of 5 min of the soak. It demonstrated air and thermal leakage paths (pointed by the red arrow) above the front bonnet. The convective heat transfer coefficients near the engine block region computed from the CFD were in the range of between 5 to 25 W/(m²K), shown in figure 6, which were of similar values at the 30 min of the soak.

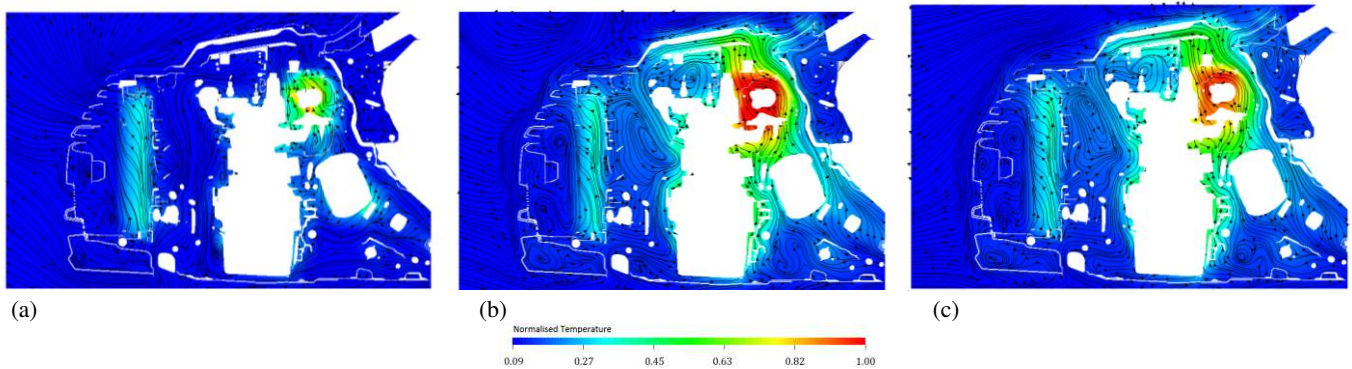


Fig. 4 Streamlines of the internal and external flow around the engine bay superimposed on the flow temperature contour at (a) 0 s, (b) 5 min and (c) 10 min of the vehicle soak

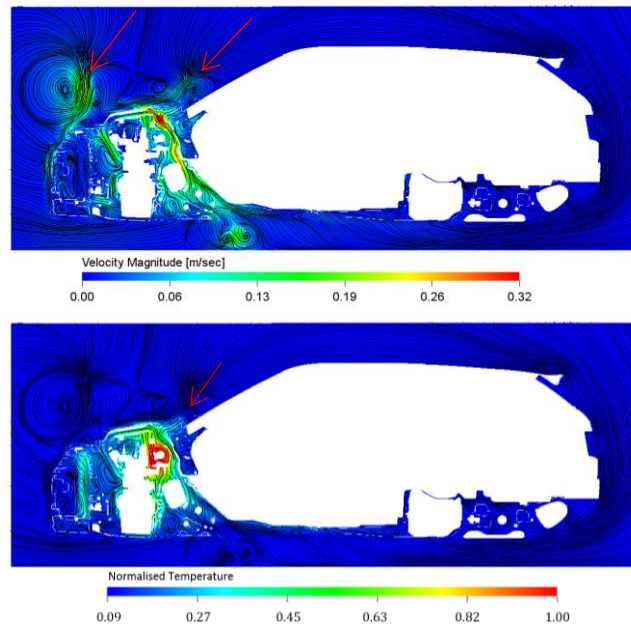


Fig. 5 Flow field (top) and normalised fluid temperature (bottom) visualisation around the engine bay at 5 min of the vehicle soak (arrow points potential leak paths)

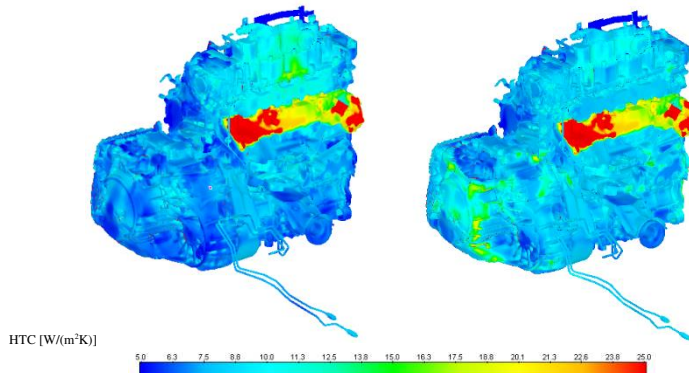


Fig. 6 Boundary conditions of the external HTCs (colour map unit: $W/(m^2K)$) around the engine block computed from CFD at the 5 min (left) and 30 min (right) of the soak

3.2. Comparison of CAE results and testing data for key fluids

The cool-down behaviours of the under-bonnet region for the 9 hrs duration of the vehicle soak were simulated by the joint coupled transient and fast standalone thermal transient modelling, the latter using the output of external HTCs and mass flow rates computed from CFD at the end of the coupled transient time period. The simulated cool-down curves of the coolant temperatures of the engine head, block, and of oil temperatures at the engine oil sump and transmission oil sump were plotted against the test data shown in figure 7. The CAE predictions of the cool-down behaviours of the key fluids were successful. The cool-down trajectories were well predicted for all four fluids of the complete 9 hrs soak period. The fluids end temperatures matched closely to the test results with the temperature difference ΔT within $1^\circ C$.

In the beginning of the soak (up to 2 hours), there is a deviation from the fluids temperatures predicted by CAE compared with the fluids sampled in the test. In the coupled simulation, single fluid node was used for calculating the heat transfer in between the corresponding engine mass to the internal fluids within. This method was successful for the engine coolants' heat transfer correlations in comparison with the test results, as the derivation between the testdata and CAE prediction was negligible throughout the 9-hr soak. However, for the prediction of oil temperatures in the engine oil sump and transmission oil sump, the method didn't model to the details of the 3D geometry of the components, the additional buoyancy-driven convection effect occurred in the oil sump especially at the early soak stage was not resolved in the current method. The temperature stratification in the oil sumps were not reflected from the single node model. Thus, there is a derivation from the averaged oil temperature from the CAE compared with the test one, which was sampled at the bottom layer of the oil in the sumps. Future work would be beneficial to take account the buoyancy effect occurred in the oil sumps to reflect the possible stratifications of oil temperatures.

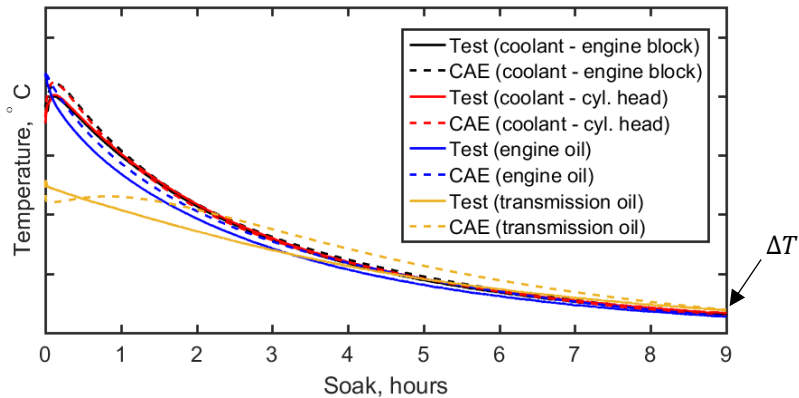


Fig. 7 Comparison of the fluids cool-down curves between CAE and test data for the coolant and oil (ΔT of the coolant block, head, engine oil and transmission oil final temperature at the end of the 9 hrs soak compared to the test data was $0.4, 1.0, 0.1$ and $0.2^\circ C$ respectively)

3.3. Sensitivity of the coupling time (external conditions) and internal HTCs

To investigate the effect of coupled simulation durations on the cool-down behaviours predictions, a series coupled transient flow-heat transfer modelling were carried out using CFD and the thermal solver for a set of time durations. The external heat transfer coefficients and surrounding air mass flow rate around the engine bay were averaged for 60 seconds (physical time) at the several timeframes (t_{couple}) from the coupled simulation results and imported separately to the standalone thermal transient (fast transient) simulation as the boundary conditions of the standalone 9 hrs cool-down simulation. The complete 9 hrs cool-down

curves calculated based on the corresponding boundary conditions from these coupled CFD results were shown in figure 8 for the engine block coolant and engine oil. The coupled timeframes examined here were 3 min, 10 min, 17 min and 30 min. It suggests that during the soak stage (0-9 hrs) the temperature differences predicted by the fast simulation compared with the test data were overall lower for the longer coupling time cases, with peak differences at the early stage of the soak (2-4 hrs). The predicted fluid temperatures at the end of the soak period were very similar. However, a shorter coupling time maybe preferred due to the much lower computing costs required. In the current study, the computing costs for simulating the 5 min and the 30 min (physical times) coupled transient simulation were 13 hrs and 53 hrs (\times 384 CPUs), respectively. This will be added upon the additional computing time used for obtaining the steady state solution - 48 hrs (384 CPUs), and for the followed fast thermal transient simulation - 3 hours (8 CPUs). The total simulation time used for the complete soak transient thermal simulation was 23,652 CPU hours, which was reduced to less than one-tenth of the computing resources used in the similar scale work reported previously in [10].

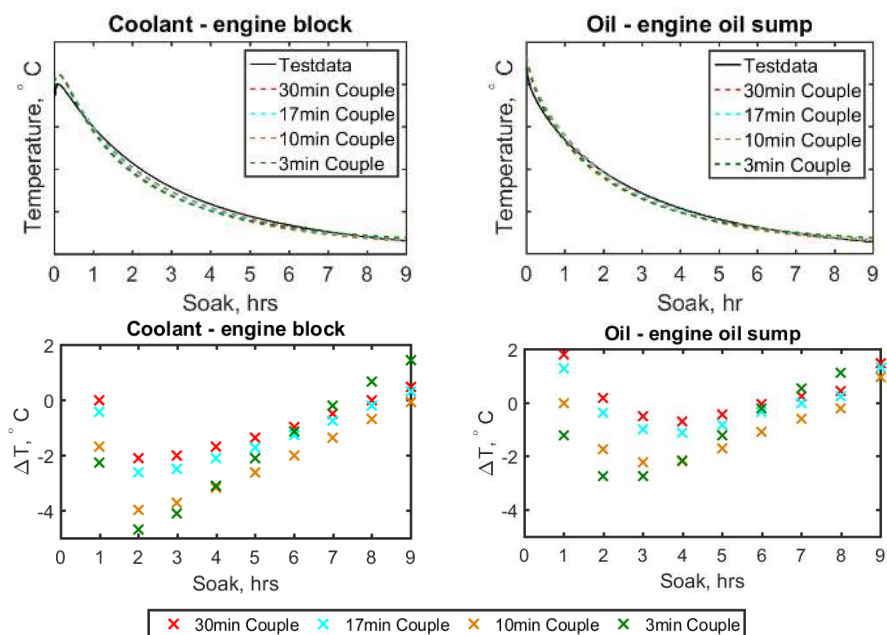


Fig. 8 Comparison of the fluids cool-down curves (top row) between the CAE (dash lines) results and the test data (solid lines) and the temperature differences ΔT compared with the test data (bottom row) with the various coupling times: 3 min, 10 min, 17 min and 30 min (i.e. with various external HTC's and mass flow rates), plotted for the coolant (left) and oil (right), respectively

Data from a correlated 1D GT-SUITE model was used for the internal HTC values, i.e. the HTC's in between the metal parts to the coolant and oil fluid nodes. To address the sensitivity of the internal HTC's to the simulated cooldown behaviours, the CAE results were also examined with the various internal fluids HTC's of fix values or pre-defined curves (in the range of 5 – 400 W/(m²K)) for both coolant and oil. It was found that the final temperature predictions were not sensitive to the internal HTC values assigned. The external HTC's were imported from CFD results as discussed previously.

3.4. Heat flux contribution analysis – Radiation, convection vs conduction effect

The calculated net heat rates contributed from conduction, convection and radiation to the engine parts' surfaces were averaged from the CAE results and plotted in figure 9 for the cylinder head, engine block and oil sump, respectively, of the 9 hrs soak duration. The net values were normalised by the maximum net values among the three heat transfer mechanisms (conduction, convection and radiation) for each of engine surfaces (engine block, cylinder heat and oil sump) separately for comparison. Convection was the main heat contribution at the early stage of the soak (0-2 hrs), for all the three engine parts: oil sump, engine block and cylinder head. At the early stage of the soak (0-4 hrs), radiation heat flux rates from the adjacent heat sources, e.g. exhaust and turbo charger unit, to the cylinder head surface were in the same order as the convection and conduction. Radiation also took a major heat contribution to the engine block transient thermal process at the early stage of the soak. However, for the oil sump, the radiation effect was relative small compared with the other two contributors, which had less than a third of the net heat rates of the other two sources. At the later stage of the soak (5-9 hrs), conduction took the major role in the heat transfer contribution and the radiation heat rates were negligible for all three parts of the engine body. The results suggested that the convection and radiation are important to be accounted of, especially at the early soak stage, in order to accurately predict the heat cool-down behaviours of the engine body and the cool-down behaviours of the internal fluids (i.e. coolant and oil).

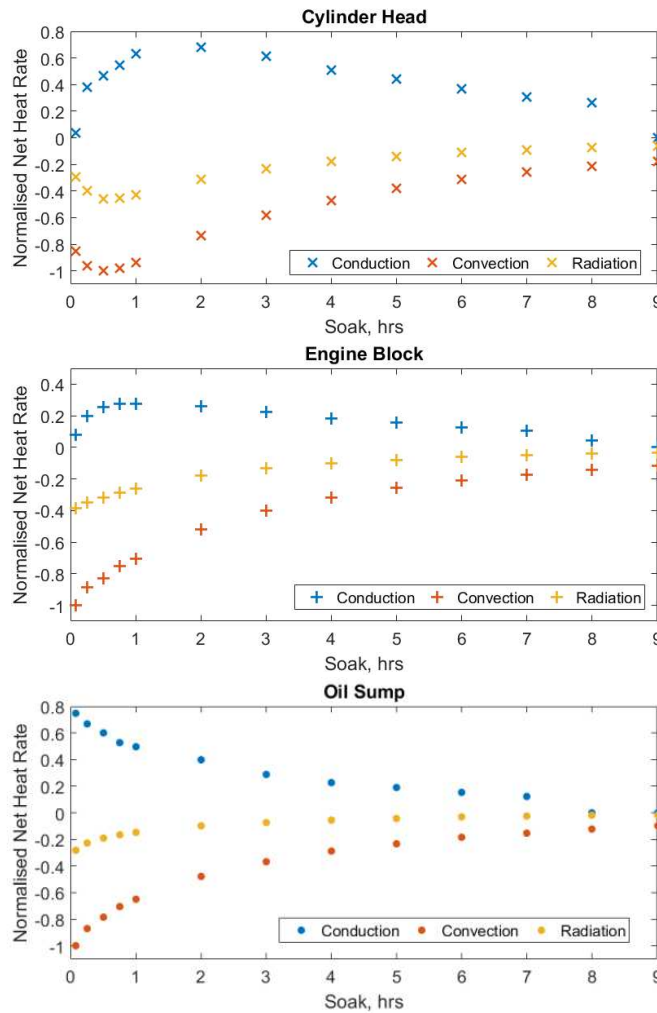


Fig. 9 Comparison of the normalised net heat rates contribution by conduction, convection and radiation to the cylinder head, engine block and engine oil sump, during the 9 hrs vehicle soak

4. CONCLUSION

Method development has been investigated in this study on a light-duty passenger vehicle using coupled aerodynamic-heat transfer thermal transient modelling method for the full vehicle under 9 hours thermal soak. The 3D buoyancy-driven under-bonnet flow dynamics were solved inherently transient by the LBM method using CFD. This was further coupled with heat transfer modelling using a thermal solver. The particle-based LBM method was capable of accurately handling extremely complicated transient flow behaviour on complex surface geometries. The detailed thermal modelling including heat conduction, radiation and buoyancy-driven heat convection were integrated solved by thermal solver. The 9 hrs cool-down was simulated and compared with the vehicle testing data of the key fluids (coolant, oil) temperatures. The developed CAE method was able to predict the cool-down behaviours of the key fluids and components in agreement with the experimental data, and also visualised the air leakage paths and thermal retention around the engine bay. The differences between the predicted fluids temperatures and the testing results were within 1 °C. The total simulation time was also significantly reduced to the 1/10th of the previous study required CPU hours. The cool-down trajectories of the key components obtained for the 9 hrs thermal soak period provide vital information and basis for investigating various designs of encapsulation, allowing a fast-running model to be developed imbedded with holistic study of vehicle thermal and energy modelling and management. It was also found that the buoyancy effect as well as the radiation effect played important parts in the thermal modelling at the first stage of the 9 hrs soak and the flow development during this stage was vital to accurately predict the heat transfer coefficients for the heat retention modelling. The developed method has demonstrated the software integration for simulating buoyancy-driven heat transfer in a vehicle under-bonnet region during thermal soak with satisfied accuracy and efficient computing time. The CAE method developed will allow integration of the design of engine encapsulations for improving fuel consumption and reducing CO₂ emissions in a timely and robust manner, aiding the development of low-carbon transport technologies.

5. FUTURE WORK DISCUSSION

The correct study has demonstrated a robust CAE method for thermal analysis of the vehicle under-bonnet region, enabling the heat and flow paths visualisations and allowing the prediction the engine fluids' thermal behaviours under the 9 hrs soak condition. In the next step, this method will be used to calculate the thermal behaviours of the key fluids and engine components with a set of engine encapsulation designs. The CAE results obtained will be fed into a powertrain warm-up model to examine the corresponding CO₂ emissions and fuel consumption corresponding to each encapsulation design. Another aspect will be added in the future work, which is to investigate the nature convection effect within the oil sump region during the soak period. In the current work, the distribution of internal heat transfer coefficients due to the internal buoyancy-induced fluid flow was not spatially resolved in the modelling methodology. The heat rejection in between the wall and the oil subjects to the internal fluid temperatures distribution is to be investigated. This is especially important in terms of inconsistent level of encapsulation design on the oil sump and has an impact on prediction accuracy of the oil temperatures at the vehicle cool-down condition.

ACKNOWLEDGEMENT

R.Yuan would like to acknowledge the funding support from the Innovate UK and the Advanced Propulsion Centre (APC) for carrying out this work.

REFERENCES

- [1] The European Commission Commission Regulation (EU) no. 2017/1151 Place: InterReg
- [2] Green Car Congress. (2009). BMW Outlines Intelligent Heat Management Applications for Reducing Fuel Consumption and CO₂; New Thermoelectric Generator Unit Integrated with EGR. [online] Available at: <https://www.greencarcongress.com/2009/10/bmw-outlines-intelligent-heat-management-applications-for-reducing-fuel-consumption-and-co2-new-ther.html>
- [3] D. Petley, W. Jansen, B. Wicksteed, D. Caprioli, T. Bürgin, Pre-development validation of an engine mounted encapsulation approach on SUV vehicle as 'Eco-Innovation' by means of EU Regulation 725/2011, In: Bargende M., Reuss HC., Wiedemann J. (eds) 14. Internationales Stuttgarter Symposium. Proceedings. Springer Vieweg, Wiesbaden, 2014.
- [4] K. Chen, J. Johnson, P. Merati, and C. Davis, Numerical investigation of buoyancy-driven flow in a simplified underhood with open enclosure, *SAE Int. J. Passeng. Cars - Mech. Syst.*, vol. 6, no. 2, pp. 805–816, 2013.
- [5] M. Franchetta, T. Bancroft, and K. Suen, Fast transient simulation of vehicle underhood in heat soak, *SAE Tech. Pap.*, 2006-01-1606, 2006.
- [6] P. Merati, C. Davis, K. Chen, and J. Johnson, Underhood buoyancy driven flow - an experimental study, *ASME, J. of Heat Transfer*, vol. 133, Aug. 2011.
- [7] B. Minovski, L. Lofdahl, and P. Gullberg, Numerical investigation of natural convection in a simplified engine bay, *SAE Tech. Pap.*, 2016-01-1683, 2016.
- [8] B. Minovski, L. Lofdahl, and P. Gullberg, A 1D method for transient simulations of cooling systems with non-uniform temperature and flow boundaries extracted from a 3D CFD solution, *SAE Tech. Pap.*, 2015-01-0337, 2015.
- [9] B. Minovski, J. Andrić, L. Lofdahl, and P. Gullberg, A numerical investigation of thermal engine encapsulation concept for a passenger vehicle and its effect on fuel consumption, *Proc IMechE Part D: J Automobile Engineering*, vol. 233, no. 3. pp. 557-571, 2019.
- [10] R. Owen, A. Price, J. D. B. Boletto, S. Sivasankaran, and W. Jansen, Method development and application of thermal encapsulation to reduce fuel consumption of internal combustion powertrains, *SAE Tech. Pap.*, 2019-01-0902, 2019.
- [11] Exa Corp., PowerFLOW User's Guide 3.0 (Exa Corp., Lexington, MA, 1998).
- [12] P. L. Bhatnagar, E. P. Gross, and M. Krook, A model for collision processes in gases. I. Small amplitude processes in charged and neutral one-component systems, *Phys. Rev.* vol. 94. Pp. 511–525, 1954.
- [13] D. P. Lockard, L. S. Luo, S. D. Milder, and B. A. Singer, Evaluation of PowerFLOW for aerodynamic applications, *J Statistical Physics*, Vol. 107, Issue 1–2. Pp. 107: 423, 2002.
- [14] RadTherm training manual, © 2014 ThermoAnalytics, Inc.